Title:

Experimental study of hexagonal and square diesel particulate filters under controlled and uncontrolled catalyzed regeneration

Authors:

Koji Tsuneyoshi* [a,b] and Kazuhiro Yamamoto [b]

Affiliation:

[a] Environmental Materials R&D Center, TYK Corporation
3-1 Ohbata-cho, Tajimi-shi, Gifu 507-8607, Japan
[b] Department of Mechanical Science and Engineering, Nagoya University
Furo-cho, Chikusa-ku, Nagoya-shi, Aichi 464-8603, Japan

Type of article:

Full length article

Address of the corresponding author

Environmental Materials R&D Center, TYK Corporation
3-1 Ohbata-cho, Tajimi-shi, Gifu 507-8607, Japan
telephone number: +81-572-25-7181
fax number: +81-572-25-6833
e-mail: ku.tsuneyoshi@tyk.jp

Abstract

Although diesel engines have high thermal efficiency, large amounts of particulate matter (PM) including soot are emitted. A wall-flow diesel particulate filter (DPF) is one of the most important technologies for diesel emission control. However, the soot accumulation inside the DPF causes an increase of pressure loss. Then, the accumulated diesel soot needs to be burned, which is called a filer regeneration process. In this study, we have investigated the soot combustion on bare and catalyzed DPFs under controlled and uncontrolled regeneration. Two types of DPFs with conventional square and hexagonal cells were used. Results show that, in comparison with the bare DPF, the regeneration efficiency of the catalyzed DPF is clearly higher, indicating a marked effect of catalysts. Independent of regeneration temperature, a greater increase in the regeneration efficiency of the catalyzed DPF was confirmed under controlled regeneration. On the other hand, under uncontrolled regeneration, the maximum temperature of the catalyzed DPF is higher than that of the bare DPF, and it is reached shorter times. Interestingly, by comparing the conventional square cell DPF, the soot oxidation of the hexagonal cell DPF is promoted under controlled and uncontrolled regeneration.

Key words:

Catalytic combustion; Soot; Oxidation; Diesel particulate filter; Regeneration

1. Introduction

Diesel engines have high thermal efficiency, lower fuel consumption, and lower CO_2 emissions, compared with equivalent gasoline engines [1]. On the other hand, diesel engines emit NOx and large amounts of particulate matter (PM) including soot in the exhaust gas. The fine particles (i.e. <2.5 mm, referred to as PM2.5) cause environmental pollution and are potentially harmful to human health [2]. Therefore, various technologies have been investigated for the reduction of diesel emission. For example, the improvement of the fuel injection with the so-called common rail [3,4] and the exhaust gas recirculation (EGR) [5,6] are known as effective technologies of PM and NOx reduction.

Under the current regulations, we do not have to care about very fine nanoparticles, because their mass is extremely low. However, if the regulation is set based on the particle number, these nanoparticles should be removed as well [7]. Therefore, a diesel particulate filter (DPF) is one of the important technologies for this type of PM regulation.

Typically, the DPF has a monolithic wall-flow structure made of ceramic. The DPF has many flow channels, which are called cells, and the porous ceramic walls act as a filter. Figure 1 shows a schematic of the wall-flow DPF. The PM is trapped on the surface of the filter wall when the exhaust gas passes through the filter. The filtration efficiency

reaches approximately 100 % after a thin soot layer is formed [8,9]. At the same time, the pressure loss increases due to formation of the soot layer (soot cake) [10,11]. This is because the inner structure of the DPF is changed by the soot accumulation, so that the flow as well as the pressure inside the DPF cell is changed [8,12]. Consequently, the fuel consumption becomes worse and the engine may stall. Then, for the reduction of the filter back pressure, the accumulated diesel soot inside the DPF must be burned, which is called filter regeneration. As for the DPF performance, high filtration efficiency, low pressure loss, and regeneration at low temperature [13] are demanded.

Normally, the exhaust gas temperature is insufficient to regenerate the filter, and a catalyst is usually used to reduce the PM oxidation temperature [14]. So far, a catalyzed DPF has been investigated for efficient DPF regeneration by soot combustion [15,16]. Although the catalyzed DPF is efficient for soot combustion, a higher pressure loss is observed in comparison with a bare DPF due to the washcoat for catalysis support [9]. For alternative approaches, several kinds of fuel additives have been used for the diesel smoke reduction [17,18]. However, the fuel additive increases the amount of ash that remains after soot burning, resulting in an increase of pressure loss [19]. Therefore, the DPF needs to have low pressure loss even when the soot and ash accumulate.

One of the solutions for the reduction of pressure loss is to change the cell

structure of the DPF. As seen in Fig. 1, the square cell is used in a commercially available DPF, which is generally a worldwide standard because of easier manufacturing and lower cost. It is known that the capacity for soot and ash depositions inside the DPF can be improved by increasing the aperture ratio of the inlet cell to the outlet cell. In this case, the pressure loss during soot loading is lower, because the soot cake is thinner, while the ash capacity is higher [19,20].

Amirnordin et al. [21] and Segawa et al. [22] have investigated a honeycomb monolith with hexagonal cells, and have reported that its pressure loss is relatively lower. However, they have focused on catalytic converters. The effect of the cell structure on the soot combustion in the DPF regeneration process is not clear. In our previous study [23], using hexagonal cell and conventional square cell DPFs, we reported that the initial PM filtration efficiency can be improved with lower pressure loss during soot loading by increasing the inlet aperture ratio.

In this study, we examine the soot combustion with catalysts in DPF regeneration. The bare and catalyzed DPFs of hexagonal and conventional square cell structures are experimentally investigated. Two types of filter regeneration are considered. One is a controlled regeneration test for soot burning at constant temperature [24]. The other is an uncontrolled regeneration test with rapid soot combustion, which is called drop-to-idle test

(DTIT) [25]. Based on experimental results, the effect of catalysts on the soot oxidation in different cell DPFs is presented and discussed.

2. Experimental setup

2.1. Characteristics of the diesel particulate filters

Four silicon-carbide (SiC) DPF samples, HEX bare, SQ bare, HEX catalyzed, and SQ catalyzed, were used in this study. The catalyzed DPFs were coated with Pt. The sample specifications are shown in Table 1. The cell structure of hexagonal and square cell bare DPFs are shown in Fig. 2. Each has the same size of Φ 144 mm × L 153 mm. The cell density is 300 cpsi, and the wall thickness is 0.25 mm. Samples HEX bare and HEX catalyzed have hexagonal cells, and samples SQ bare and SQ catalyzed have conventional square cells. The inlet aperture ratio of the hexagonal cell DPF is 46.2 %, which is larger than 34.2 % of the square cell DPF. The pore structure characteristics were measured by mercury porosimetry (Micromeritics Co. AutoPore 9500). The porosity and the average pore diameter of HEX bare and SQ bare were approximately 46 % and 16 μm.

2.2. Controlled regeneration test

In general, for the DPF regeneration, the accumulated soot inside the DPF is

burned using the exhaust gas under high engine speed [24]. Then, the controlled regeneration test was conducted by an engine test bench with a Nissan QD32 diesel engine. Each sample was loaded with 8 g/L soot in advance. A schematic of the experimental setup is shown in Fig. 3. Table 2 shows the engine specifications, and Table 3 shows the properties of diesel fuel used in this study. The engine was connected to an eddy current dynamometer (Tokyo Plant Co. ED-150) to set the test condition with 1400 rpm and 190 N･m load for soot loading. A diesel oxidation catalyst or DOC (ACR Co. EXCAT C15) was placed upstream of the DPF.

In order to burn the soot for filter regeneration, the temperature and the oxygen concentration of exhaust gas were kept constant for 30 min [24]. The amount of burned soot and the regeneration efficiency were calculated based on the DPF weight after the regeneration test. As shown in Fig. 4, twelve K-type thermocouples were inserted into the DPF channels from the outlet side of the DPF to measure the temperature inside the DPF. Three sets of four thermocouples each were positioned at 4, 34, and 64 mm from the DPF axis. The four thermocouples of each set were placed at 15, 30, 75, and 120 mm distance from the DPF outlet. We controlled the DPF regeneration temperature by the thermocouples of ch 7. We measured the oxygen concentration using an oxygen sensor (Cosmos Co. XP-3180E). Three conditions were selected at different regeneration

temperatures of 510, 550, 590 °C at engine speed of 3000 rpm. The oxygen concentrations were 9.4, 8.2, 7.2 % by volume. These test conditions are shown in Table 4.

2.3. Uncontrolled regeneration test

Normally, the uncontrolled regeneration test is conducted to evaluate the thermal stress caused by the rapid soot combustion inside the DPF, which is totally different from the controlled regeneration situation. This could be a failure scenario for filter regeneration. It could be caused by a sudden vehicle braking with the engine operating at high load and speed, resulting in an onset of very fast regeneration due to the combination of high temperature, low exhaust flow rate, and high oxygen content. In this case, the unexpectedly fast regeneration would lead to much higher temperatures, possibly damaging the DPF. Thus, the information on this kind of failure scenario is quite valuable [15]. In the experiments, the soot loaded DPF connected to an exhaust pipe was heated by exhaust gas under conditions of 3000 rpm (full throttle) followed by setting the engine at idle speed (750 rpm, 0 N·m) as soon as the temperature measured by the thermocouples of ch 7 reached 680 °C. Thus, it is called drop-to-idle test (DTIT) [25]. It should be noted that the soot is hardly burned in conditions with full throttle, because the volumetric oxygen concentration is very low (typically, 2 % by volume). However, at the engine idle

speed, the soot burns rapidly because the exhaust gas contains more oxygen (19 % by volume). Similar to the controlled regeneration test, the DPF temperature was measured by thermocouples. The regeneration efficiency was calculated based on the DPF weight after the test. The loaded soot amount in the DPF was 6 or 8 g/L.

3. Results and discussion

3.1. Controlled regeneration test

Figure 5 shows the variations of the temperature inside the DPF and the back pressure (ΔP) in the controlled regeneration test. Results of hexagonal and square cell bare samples are shown, separately. The results of condition 2 are shown, where the regeneration temperature was maintained at 550 °C for 30 min. It is seen that the outer temperature of ch 11 is lower than the inner temperature of ch3 because of the heat loss toward the outside of the DPF. The back pressure gradually decreases for both samples, because the deposited soot is burned, i.e. the DPF is regenerated.

It is well known that the back pressure during soot loading increases linearly with the thickness of the soot cake [8,9]. Thus, in the filter regeneration process, as the soot cake layer is decreased, the filter back pressure is lower. Interestingly, as seen in this figure, the back pressure of the hexagonal cell DPF is lower than that of the square cell

DPF. Although only the test condition 2 is shown in Fig. 5, this tendency was also observed in test conditions 1 and 3, ensuring that the back pressure in the soot loaded DPF is lower by changing the cell structure with higher inlet aperture ratio [23].

To discuss the filter back pressure and soot deposition layer, we compare the gas flow with soot cake formation for the hexagonal and square cell DPFs (see Fig. 6). During the initial filtration, independent of cell structure, the exhaust gas flows directly from the inlet cell to the outlet cell (see “flow 1” in Fig. 6a). However, due to the increase of back pressure in the hexagonal cell DPF, the gas flows from the inlet cell to the outlet cell through the filter substrate wall (flow 2), as well as the original flow 1 [19]. In our previous study [23], it was shown that the flow 2 which is from the inlet cell to the outlet cell through the filter substrate wall could occur. Consequently, in the case of the hexagonal cell DPF, the soot cake could be wider and thinner with lower back pressure, because the hexagonal cell DPF has a larger aperture ratio and a larger filtration area.

Figure 7 shows SEM images of the soot cake regions of sliced hexagonal and square cell DPFs with 8 g/L soot loading. The thickness of the soot layer is shown in these images at different positions. It should be noted that, as seen in Fig. 7a, the soot cake of the hexagonal cell DPF is formed on the wall of the inlet and inlet cells. The average thickness of the soot cake of the hexagonal cell DPF is 117 μm, which is smaller than 136

μm of the square cell DPF. Thus, the back pressure of the hexagonal cell DPF is lower than that of the square cell DPF.

Figure 8 shows the comparison of the time variation of back pressure for each sample in controlled regeneration test (test condition 2). Since the temperature profiles in the catalyzed DPF are almost the same in Fig.5, the time variation of temperature is omitted. It is seen that, independent of cell structure, the peak back pressure of the catalyzed sample is slightly higher than that of the bare sample. This is due to the lower porosity of the catalyzed DPF [9,20]. However, the back pressures of both catalyzed samples decrease rapidly, and are lower than those of the bare samples. It is considered that the soot burning is promoted by the catalyst.

After 1300 s, the back pressure of square cell catalyzed sample is smaller than that of hexagonal cell catalyzed DPF. It should be noted that the initial (no soot loading) back pressure of the square cell DPF is lower than that of the hexagonal cell DPF [23]. Therefore, the back pressure of the square catalyzed DPF could be lower than that of the hexagonal catalyzed DPF, if the accumulated soot burns to some extent.

In order to evaluate the catalytic effects of different cell structures, we examined the filter regeneration efficiency [9,23], which was calculated from:

$$regeneration\ \ efficiency\ = \left(\frac{M_1}{M_0}\right)\times 100 \qquad (1)$$

where M_0 is the initial amount of loaded soot before regeneration, and M_1 is the amount of burned soot during regeneration. Results at different DPF regeneration temperatures are shown in Fig. 9. It is seen that, for all samples, the regeneration efficiency is increased with an increase of the regeneration temperature. Song et al. [26] have reported a relationship between the DPF inlet temperature and the back pressure during regeneration. More soot is burned during DPF regeneration when the oxygen concentration is increased. In our previous study [27,28], the effect of the oxygen concentration was also examined in the numerical simulation, showing that the soot oxidation is substantially promoted at higher oxygen concentration. However, as seen in Table 2, when the DPF regeneration temperature is higher, the oxygen concentration is lower. Thus, in the controlled regeneration test, more soot is burned at higher regeneration temperature, even if the oxygen concentration is lower.

As seen in Fig. 9, for both the hexagonal and square cell DPFs, the regeneration efficiency of catalyzed DPFs are clearly higher, indicating a marked effect of the catalyst. In particular, a greater increase in the regeneration efficiency for the catalyzed sample is

seen at lower regeneration temperatures of 510 °C and 550 °C. Additionally, independent of the DPF regeneration temperature, the regeneration efficiency of the hexagonal cell DPF is higher than that of the conventional square cell DPF. Although the difference between square and hexagonal cell DPFs in Fig. 9 is small, the tendency was not changed even if the DPF regeneration temperature is varied. Therefore, for catalyzed or non-catalyzed DPF, the regeneration efficiency of the hexagonal cell DPF can be higher.

It is also important to consider the contact area between exhaust gas and soot deposition layer, because the soot oxidation rate is determined by the oxygen supply. As shown in Figs. 6 and 7, the hexagonal cell DPF has a large soot accumulation area because of the larger inlet aperture ratio, compared with the square cell DPF. Hence, more soot reacts with oxygen in the case of the hexagonal cell DPF. Thus, independent of the regeneration temperature, the regeneration efficiencies of the hexagonal cell DPFs are higher than those of the square cell DPFs.

3.2. Uncontrolled regeneration test

Next, the uncontrolled regeneration drop-to-idle-tests (DTIT) were performed. This test simply models the situation where the fuel dosing is stopped with more oxygen supply in the diesel engine combustion. In this case, the temperature inside the DPF could

be extremely higher. Figure 10 shows the comparison of the regeneration efficiency for each sample, at different soot loads. The accuracy of the regeneration efficiency was evaluated in several tests. The error in regeneration efficiency in DTIT was 3 % or less. In Fig. 10, it is seen that the regeneration efficiency is higher as more soot is accumulated (8 g/L). As for the non-catalyzed DPF, the regeneration efficiency of the hexagonal cell DPF is higher than that of the square cell DPF, which is the same trend in the controlled regeneration test. This could be due to the larger contact area, so that the soot is reacted with more oxygen in the hexagonal cell DPF. However, in the case of catalyzed samples, smaller difference in regeneration efficiency is observed between the hexagonal and square cell DPFs. Even for the 6 g/L soot loaded DPF, the regeneration efficiency reaches approximately 90 %. Thus, the soot oxidation is largely promoted by the catalyst, and a smaller effect of cell structure is observed.

The temporal variation of the DPF temperature during the DTIT is shown in Figs. 11 and 12 for soot loads of 6 g/L and 8 g/L, respectively. The temperature was measured by the K-type thermocouples with no value over 1300 °C obtained. Independent of the measuring position, the maximum temperature of the catalyzed DPF is higher than that of the bare DPF. Additionally, the time to reach maximum temperature can be shorter. Although the temperature is higher for the 8 g/L soot loaded sample, the above-mentioned

tendencies are also observed in Fig. 12. This is because the soot combustion is largely promoted by the catalyst.

Figure 13 shows the relationship between the burned soot amount and the maximum temperature. In the case of catalyzed samples with 8 g/L loaded soot, the maximum temperature was over 1300 °C. It is found that the maximum temperature of the catalyzed DPF is approximately 200 °C higher than that of the bare DPF. Interestingly, regardless of the bare or catalyzed DPF, the maximum temperature increases linearly as more soot is burned. This is simply because the maximum temperature depends on the burned soot, and is independent of the loaded soot amount.

In the case of the 8 g/L DTIT in Fig. 12, the peak temperature of the hexagonal cell bare DPF is larger than that of the square one. That is, when the burned soot amount is the same, the maximum temperature of the hexagonal cell DPF is lower. Note that, in the case of the hexagonal cell DPF, the maximum temperature could be reduced when the amount of burned soot is the same. From this point of view, in comparison with the conventional square cell DPF, the hexagonal cell DPF has better thermal durability. In other words, when the hexagonal cell structure is adopted, lower thermal stresses develop inside the DPF under uncontrolled regeneration.

4. Conclusions

We have investigated the soot combustion (oxidation) under controlled and uncontrolled regeneration, by using catalyzed or bare hexagonal and conventional square cell DPFs. From the results obtained, the following conclusions may be drawn:

1. In the case of the hexagonal cell DPF, the soot oxidation is enhanced, and the regeneration efficiency is higher under controlled regeneration. Since the hexagonal cell DPF has a larger filtration area, the soot cake can be thinner. Therefore, the back pressure of the hexagonal cell DPF with soot cake is lower than that of the square cell DPF. Although the peak back pressure of the catalyzed DPF is higher, the back pressure decreases rapidly compared with that of the bare sample.
2. Under uncontrolled regeneration (DTIT), in the case of catalyzed samples, the time to reach maximum temperature can be shortened, with higher maximum temperature values. Regardless of the bare or catalyzed DPF, the maximum temperature increases linearly as more soot is burned. This is simply because the maximum temperature depends on the burned soot amount.
3. For all samples, the regeneration efficiency in the DTIT test is higher as more soot is accumulated. The maximum temperature is lower in the case of the hexagonal cell DPF at the same amounts of burned soot. Therefore, in comparison with the

conventional square cell DPF, the hexagonal cell DPF has better thermal durability under uncontrolled regeneration.

References

[1] Yezerets A, Currier WN, Kim HD, Eadler AH, Epling SW, Peden HFC, Differential kinetic analysis of diesel particulate matter (soot) oxidation by oxygen using a step-response technique. Applied Catalysis B: Environmental 2005;61:120-9.
[2] Kennedy IM, The health effects of combustion-generated aerosols. Proceedings of the Combustion Institute 2007;31:2757-70.
[3] Knecht W, Diesel engine development in view of reduced emission standards. Energy 2008;33(2):264-71.
[4] Torregrosa AJ, Broatch A, Novella R, Mónico LF, Suitability analysis of advanced diesel combustion concepts for emissions and noise control. Energy 2011;36(2): 825-38.
[5] Maiboom A, Tauzia X, Hétet JF, Experimental study of various effects of exhaust gas recirculation (EGR) on combustion and emissions of an automotive direct injection diesel engine. Energy 2008;33(1):22-34.
[6] Bermúdez V, Lujan JM, Pla B, Linares WG, Effects of low pressure exhaust gas recirculation on regulated and unregulated gaseous emissions during NEDC in a light-duty diesel engine. Energy 2011;36(9):5655-65.
[7] Official Journal of the European Union, Regulation (EC) No. 595/2009, July 18; 2009.
[8] Wirojsakunchai E, Schroeder E, Kolodziej C, Foster DE, Schmidt N, Root T, Kawai T, Suga T, Nevius T, Kusaka T, Detailed diesel exhaust particulate characterization and real-time DPF filtration efficiency measurements during PM filling process. In: SAE Technical Paper 2007-01-0320; 2007.
[9] Tsuneyoshi K, Takagi O, Yamamoto K, Effects of washcoat on initial PM filtration efficiency and pressure drop in SiC DPF. In: SAE Technical Paper 2011-01-0817; 2011.
[10] Lapuerta M, Fernández JR, Oliva F, Effect of soot accumulation in a diesel particle filter on the combustion process and gaseous emissions. Energy 2012;47(1):543-52.
[11] Piscaglia F, Ferrari G, A novel 1D approach for the simulation of unsteady reacting flows in diesel exhaust after-treatment systems. Energy 2009;34:2051-62.
[12] Yamamoto K, Oohori S, Yamashita H, Daido S, Simulation on soot deposition and combustion in diesel particulate filter. Proceedings of the Combustion Institute 2009;32:1965-72.
[13] Torregrosa AJ, Serrano JR, Arnau FJ, Piqueras P, A fluid dynamic model for unsteady compressive flow in wall-flow diesel particulate filters. Energy 2011;36:671-84.
[14] Wang S, Haynes BS, Catalytic combustion of soot on metal oxides and their supported metal chlorides. Catalysis Communications 2003;4:591-6.
[15] Koltsakis GC, Stamatelos AM, Catalytic automotive exhaust aftertreatment. Progress in Energy and Combustion Science 1997;23:1-39.
[16] Yamamoto K, Nakamura M, Yane H, Yamashita H, Simulation on catalytic reaction in diesel particulate filter. Catalysis Today 2010;153:118-24.
[17] Rakopoulos DC, Rakopoulos CD, Giakoumis EG, Dimaratos AM, Characteristics of performance and emissions in high-speed direct injection diesel engine fueled with diethyl ether/diesel fuel blends. Energy 2012;43(1):214-24.
[18] Rakopoulos CD, Dimaratos AM, Giakoumis EG, Rakopoulos DC, Investigating the

emissions during acceleration of a turbocharged diesel engine operating with bio-diesel or n-butanol diesel fuel blends. Energy 2010;35(12):5173-84.
[19] Ogyu K, Ohno K, Hong S, and Komori T, Ash storage capacity enhancement of diesel particulate filter. In: SAE Technical Paper 2004-01-0949; 2004.
[20] Ogyu K, Oya T, Ohno K, and Konstandopolous GA, Improving of the filtration and regeneration performance by the SiC-DPF with the layer coating of PM oxidation catalyst. In: SAE Technical Paper 2008-01-0621; 2008.
[21] Amirnordin SH, Seri SM, Salin WSIW, Rahman HA, Hasnan K, Pressure drop analysis of square and hexagonal cells and its effects on the performance of catalytic converters. International Journal of Science and Development 2011;2(3):239-46.
[22] Segawa Y, Hase T, Yoshida T, Hexagonal cell ceramic substrates for lower emission and backpressure. In: SAE Technical Paper 2008-01-0805; 2008.
[23] Tsuneyoshi K, Yamamoto K, A study on the cell structure and the performances of wall-flow diesel particulate filter, Energy 2012;48:492-9.
[24] Lapuerta M, Oliva F, Agudelo JR, Boehman AL, Effect of fuel on the soot nanostructure and consequences on loading and regeneration of diesel particulate filters. Combustion and Flame 2012;159:844-53.
[25] Boger T, He S, Collins T, Heibel A, Beall D, Remy C, A next generation cordierite diesel particle filter with significantly reduced pressure drop. In: SAE Technical Paper 2011-01-0813; 2011
[26] Song J, Wang J, Boehman AL, Examination of the oxidation behavior of biodiesel soot. Combusttion and Flame 2006;146:73-84.
[27] Yamamoto K, Nakamura M, Takada N, Misawa M, Combustion simulation with Lattice Boltzmann method in a three-dimentional porous structure. Proceedings of the Combustion Institute 2005;30:1509-15.
[28] Yamamoto K, Yamauchi K, Takada N, Misawa M, Furutani H, Shinozaki O, Lattice Boltzmann simulation on continuously regenerating diesel filter. Philosophical Transactions A Mathematical Physical & Engineering Science 2011;369:2584-91.

LIST OF FIGURES

Fig. 1 A schematic of wall-flow diesel particulate filter (DPF).
Fig. 2 Appearance and cell structure of (a) hexagonal cell DPF, (b) square cell DPF.
Fig. 3 Experimental setup for engine test bench.
Fig. 4 Positions of thermocouples.
Fig. 5 Temporal variations of temperature inside DPF and back pressure in controlled regeneration test (test condition 2); (a) hexagonal cell bare DPF, (b) square cell bare DPF.
Fig. 6 Comparison of the gas flow with soot cake formation between (a) hexagonal cell DPF, and (b) square cell DPF.
Fig. 7 SEM images of the soot cake regions of (a) hexagonal and (b) square cell DPFs with 8 g/L soot loading.
Fig. 8 Temporal variation of back pressure on each sample in controlled regeneration test (test condition 2).
Fig. 9 Regeneration efficiency for three test conditions.
Fig. 10 Regeneration efficiency at different soot loaded amount.
Fig. 11 Temporal variation of DPF temperature in drop-to-idle test (6 g/L soot loading sample); (a) bare hexagonal cell DPF, (b) bare square cell DPF, (c) catalyzed hexagonal cell DPF, (d) catalyzed square cell DPF.
Fig. 12 Temporal variation of DPF temperature in drop-to-idle test (8 g/L soot loading sample); (a) bare hexagonal cell DPF, (b) bare square cell DPF, (c) catalyzed hexagonal cell DPF, (d) catalyzed square cell DPF.
Fig. 13 Variation of maximum DPF temperature with burned soot amount.
Table 1 Sample specifications
Table 2 Engine specifications.
Table 3 Properties of diesel fuel.
Table 4 Test conditions.

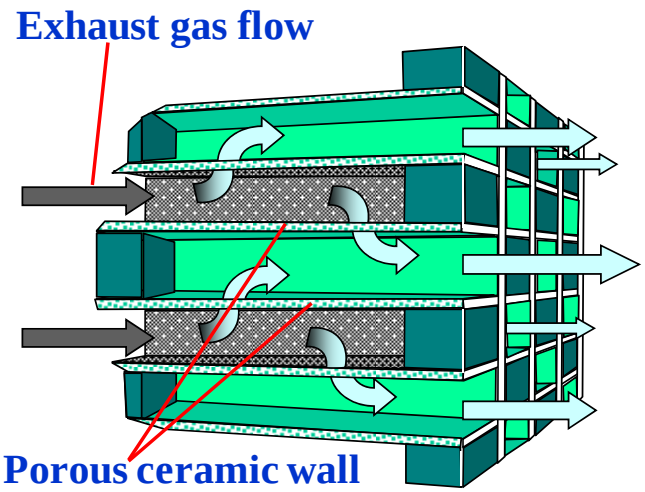

Fig. 1. A schematic of wall-flow diesel particulate filter (DPF).

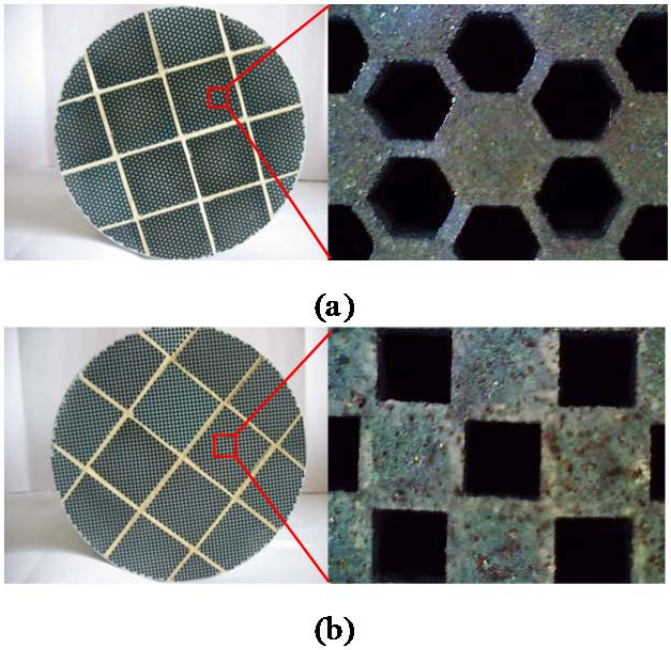

Fig. 2. Appearance and cell structure of (a) hexagonal cell DPF, (b) square cell DPF.

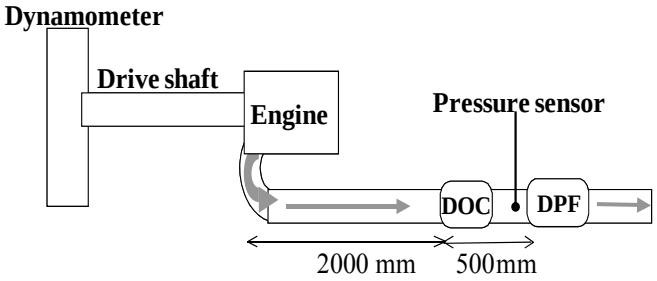

Fig. 3 Experimental setup for engine test bench.

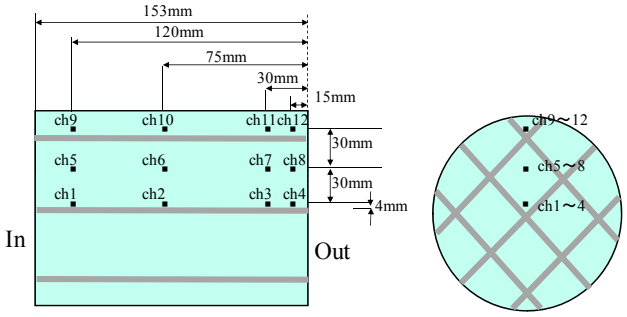

Fig. 4. Positions of thermocouples.

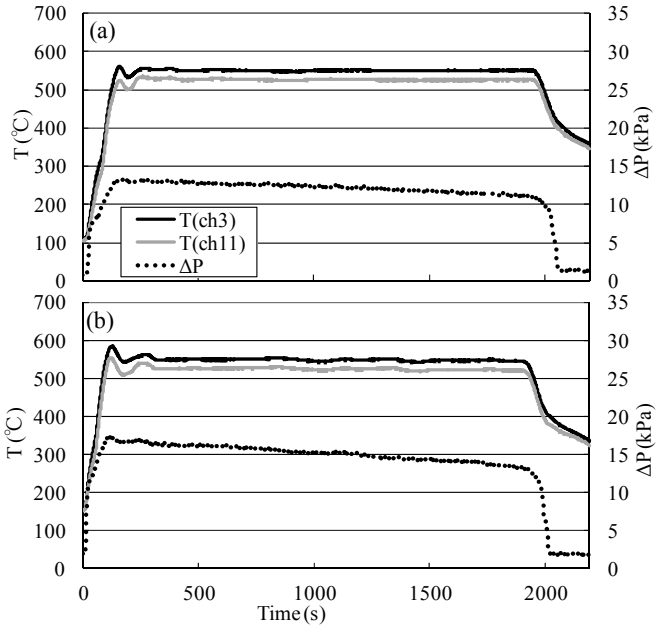

Fig. 5. Temporal variations of temperature inside DPF and back pressure in controlled regeneration test (test condition 2); (a) hexagonal cell bare DPF, (b) square cell bare DPF.

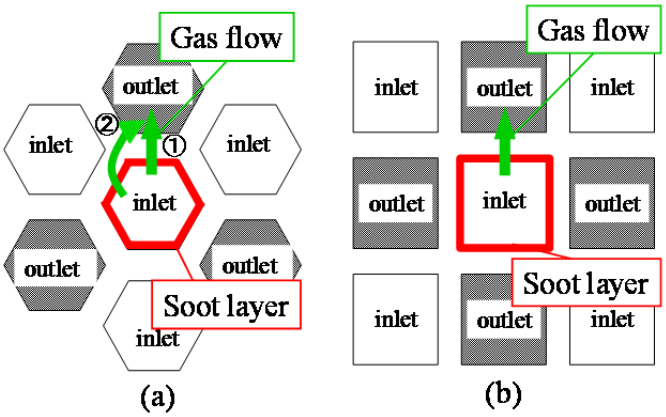

Fig. 6. Comparison of the gas flow with soot cake formation between (a) hexagonal cell DPF, and (b) square cell DPF. Flow 1 is directly from inlet cell to outlet cell, and flow 2 is from inlet cell to outlet cell through the filter substrate wall.

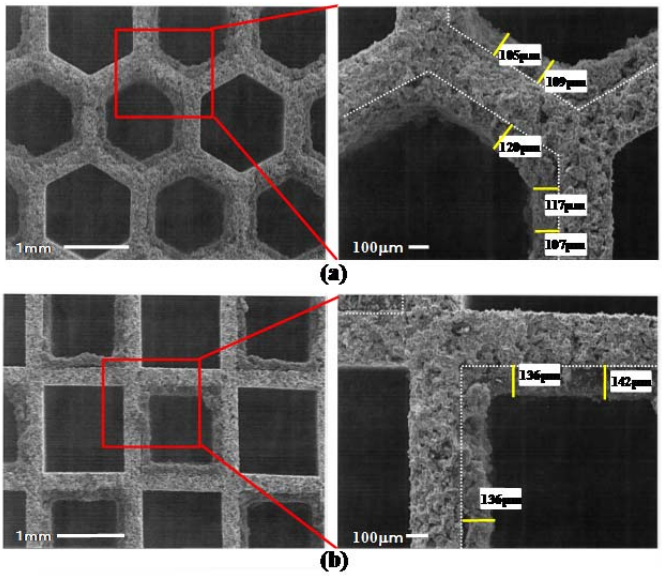

Fig. 7. SEM images of the soot cake regions of (a) hexagonal and (b) square cell DPFs with 8 g/L soot loading.

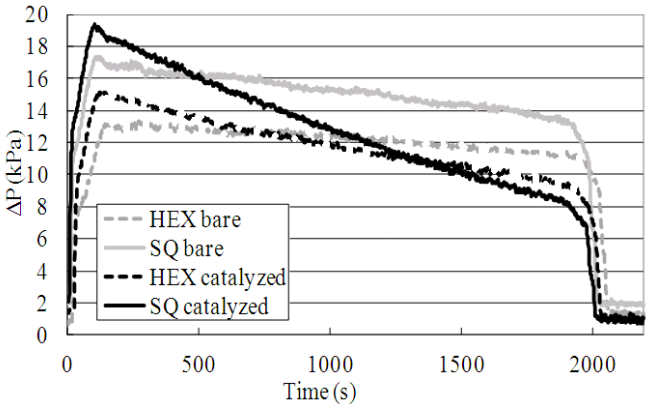

Fig. 8. Temporal variation of back pressure on each sample in controlled regeneration test (test condition 2).

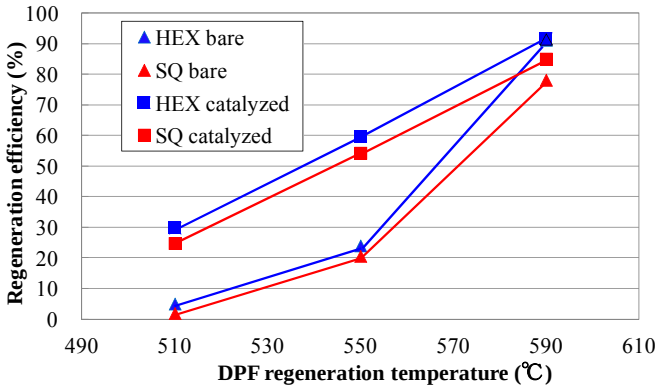

Fig. 9. Regeneration efficiency for three test conditions.

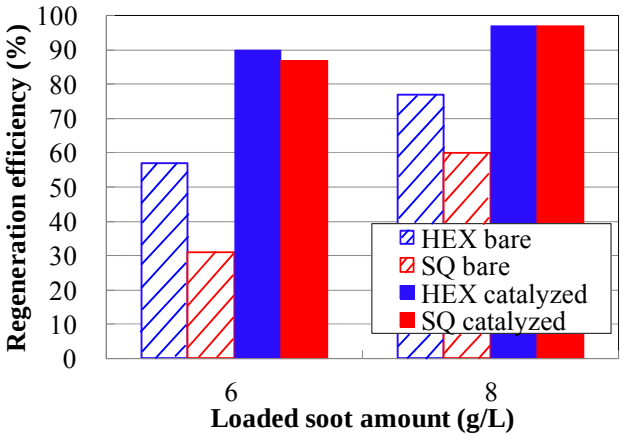

Fig. 10. Regeneration efficiency at different soot loaded amount.

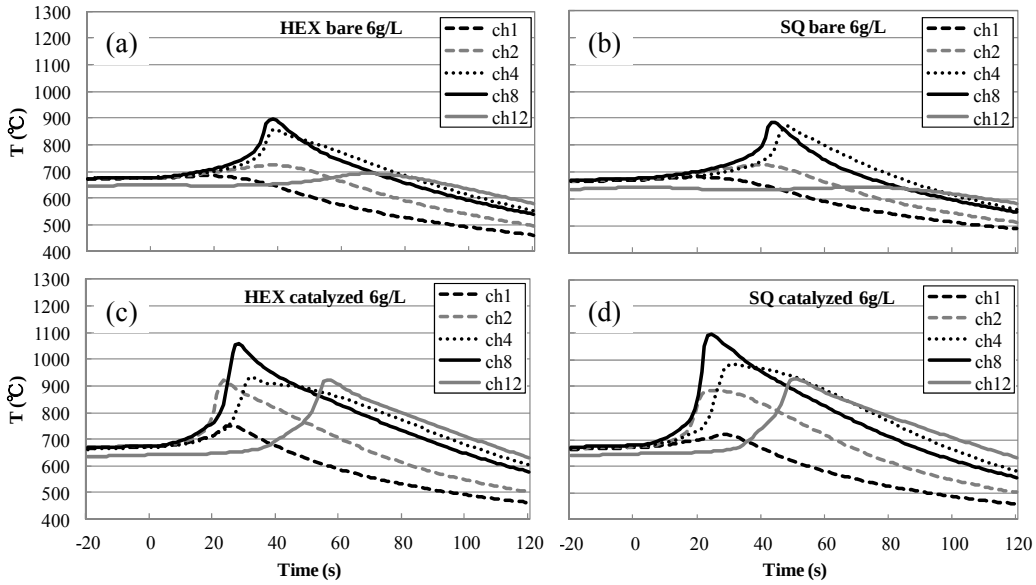

Fig. 11. Temporal variation of DPF temperature in drop-to-idle test (6 g/L soot loading sample); (a) bare hexagonal cell DPF, (b) bare square cell DPF, (c) catalyzed hexagonal cell DPF, (d) catalyzed square cell DPF.

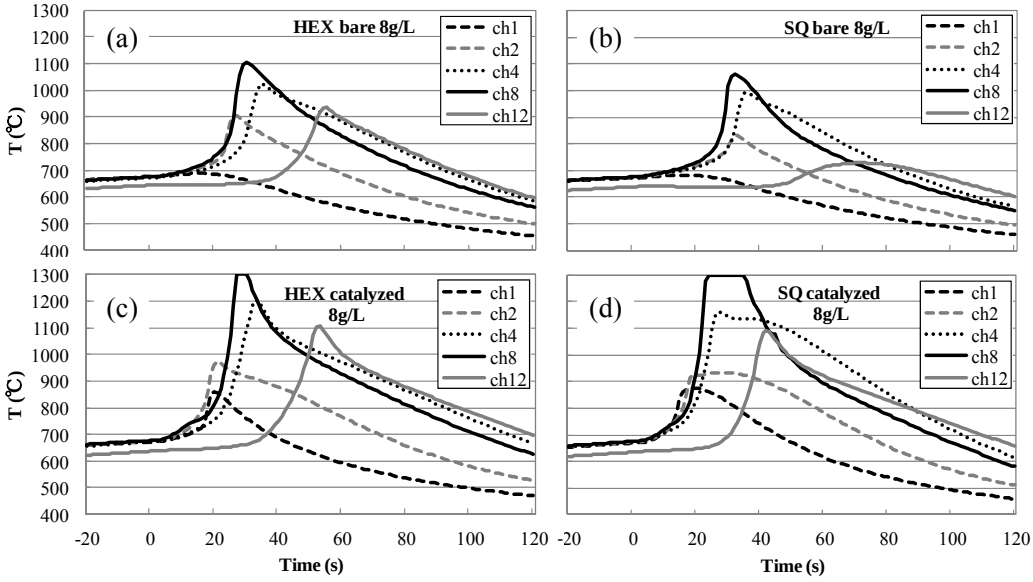

Fig. 12. Temporal variation of DPF temperature in drop-to-idle test (8 g/L soot loading sample); (a) bare hexagonal cell DPF, (b) bare square cell DPF, (c) catalyzed hexagonal cell DPF, (d) catalyzed square cell DPF.

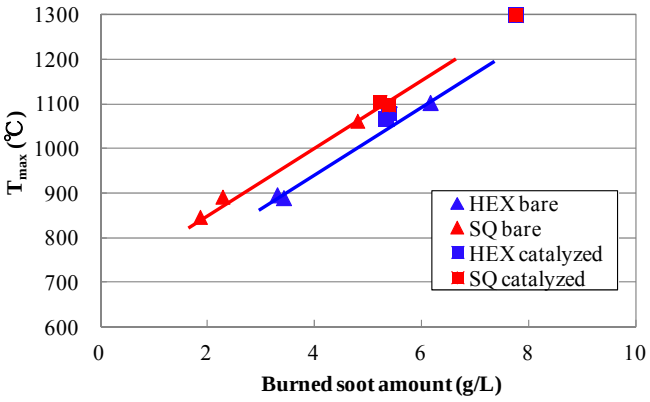

Fig. 13. Variation of maximum DPF temperature with burned soot amount.

Table 1 Sample specifications.

Sample	HEX bare	SQ bare	HEX catalyzed	SQ catalyzed
Substrate		SiC (silicon-carbide)		
Size (mm)		D144, L153		
Cell Geometry	Hexagon	Square	Hexagon	Square
Cell Density (cpsi)	300	300	300	300
Wall Thickness (mm)	0.25	0.25	0.25	0.25
Open Frontal Area (%)	46.2	34.2	46.2	34.2
Open Rear Area (%)	22.6	34.2	22.6	34.2
Porosity (%)	46.3	46.5	unknown	unknown
Average Pore Diameter (μm)	16.0	16.8	unmeasured	unmeasured
Washcoat	uncoated	uncoated	coated	coated
Pt Loading	none	none	Pt-catalyzed	Pt-catalyzed

Table 2 Engine specifications.

Model	NISSAN QD32
Engine type	4 stroke, swirl chamber, diesel
Cylinders	4, in-line
Valve mechanism	OHV
Displacement	3.153 L
Rated power	72 kW @ 3600 rpm
Peak torque	216 Nm @ 2000 rpm
EGR system	none
Turbocharger	none (naturally aspirated)

Table 3 Properties of diesel fuel.

Flash point (°C)	45 – 110
Distillation range (°C)	140 - 400
Density at 15°C (g/cm^3)	0.80 – 0.87
Sulfur content (ppm)	<10

Table 4 Test conditions.

Test condition	1	2	3
Engine speed (rpm)	3000	3000	3000
Throttle angle (%)	65	68	70
Torque (Nm)	100	110	120
Exhaust gas temp (°C)	550	600	650
Regeneration temp (°C)	510	550	590
O_2 concentration (%)	9.4	8.2	7.2